JOC Article

Crown Ether Vinylogous Tetrathiafulvalene Receptors: Complexation Interference on the Molecular Movements Triggered by Electron Transfer

Julien Massue, Nathalie Bellec, Michel Guerro, Jean-François Bergamini, Philippe Hapiot,* and Dominique Lorcy*

Sciences Chimiques de Rennes, UMR 6226 CNRS-Université de Rennes 1, Campus de Beaulieu, Bât 10A, 35042 Rennes cedex, France

dominique.lorcy@univ-rennes1.fr

Received January 30, 2007

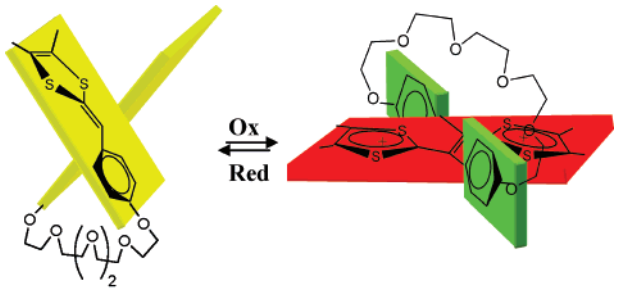

The synthesis of a series of crown ether substituted vinylogous tetrathiafulvalenes (TTFVs) has been carried out through oxidative coupling of bisdithiafulvenes. These new receptors have been fully characterized using electrochemical, spectroelectrochemical, and molecular modeling experiments. These studies show that, upon oxidation, either a clip movement (TTFVs **3a**,**b**) or a stretch movement (TTFV **3c**) occurs, depending on the length of the crown ether chains. Preliminary electrochemical studies, undertaken on TTFV **3c** in dichloromethane, show a little shift of the first standard oxidation potential toward more positive values upon addition of the Pb^{2+} ion, but a considerable variation of the electron-transfer kinetics. This result introduces an interesting concept for the preparation of sensors not based on thermodynamic variations but on kinetic modifications of the electron transfer.

Introduction

The concept of induced molecular movement has been proposed as a convenient tool for transforming chemical information to electrical information.[1−2] The design of molecular systems capable of realizing this transformation would involve a transducer such as a redox-active species for transferring the information and an easily controllable mobile unit for encoding the information. An interesting electrochemically driven motion has already been observed in the redox-active vinyloguous tetrathiafulvalene (TTFV) framework. Indeed, all the neutral TTFVs substituted (R) on the central conjugation exhibit nonplanar structures, due to steric hindrance,[3] while for the oxidized species, the TTFV cores become planar with the R substituents located in planes perpendicular to that formed by

* To whom correspondence should be addressed. Fax: (+33)-2-23-23-67-38.

(1) (a) Balzani, V.; Venturi, M.; Credi, A. *Molecular Devices and Machines: A Journey into the Nanoworld*; Wiley-VCH: Weinheim, Germany, 2003. (b) Willner, I.; Basnar, B.; Willner, B. *Adv. Funct. Mater.* **2007**, *17*, 702.

(2) For some examples of molecular motions triggered by electron transfers see: (a) *Acc. Chem. Res.* **2001**, *34*, 410−522 ("Molecular Machines" special issue). (b) Carella, A.; Coudret, C.; Guirado, G.; Rapenne, G.; Vives, G.; Launay, J.-P. *Dalton Trans.* **2007**, 177. (c) Nygaard, S.; Laursen, B. W.; Flood, A. H.; Hansen, C. N.; Jeppesen, J. O.; Stoddart, J. F. *Chem. Commun.* **2006**, 144. (d) Christensen, C. A.; Batsanov, A. S.; Bryce, M. R. *J. Am. Chem. Soc.* **2006**, *128*, 10484.

(3) (a) Hopf, H.; Kreutzer, M.; Jones, P. G. *Angew. Chem., Int. Ed. Engl.* **1991**, *30*, 1127. (b) Lorcy, D.; Carlier, R.; Robert, A.; Tallec, A.; Le, Maguerès, P.; Ouahab, L. *J. Org. Chem.* **1995**, *60*, 2443. (c) Ohta, A.; Yamashita, Y. *J. Chem. Soc., Chem. Commun.* **1995**, 1761. (d) Moore, A. J.; Bryce, M. R.; Skabara, P. J.; Batsanov, A. S.; Goldenberg, L. M.; Howard, J.A. K. *J. Chem. Soc., Perkin Trans. 1* **1997**, 3443. (e) Yamashita, Y.; Tomura, M.; Braduz Zaman, M.; Imaeda, K. *J. Chem. Soc., Chem. Commun.* **1998**, 1657. (f) Jia, C.; Liu, S-X.; Neels, A.; Stoeckli,-Evans, H. Decurtins, S. *Synthesis* **2005**, 2157. (g) Guerro, M.; Lorcy, D. *Tetrahedron Lett.* **2005**, *46*, 5499.

10.1021/jo0701841 CCC: $37.00
Published on Web 05/24/2007

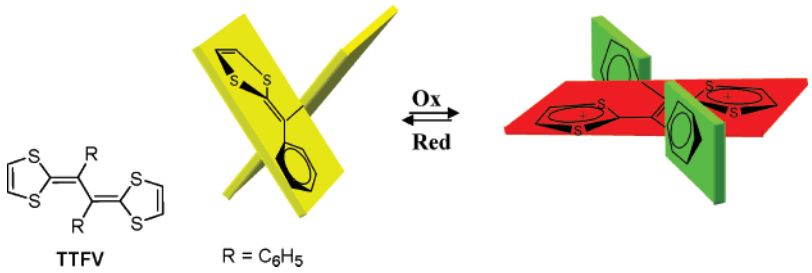

FIGURE 1. Schematic representation of the stretch movement observed with TTFVs upon oxidation.

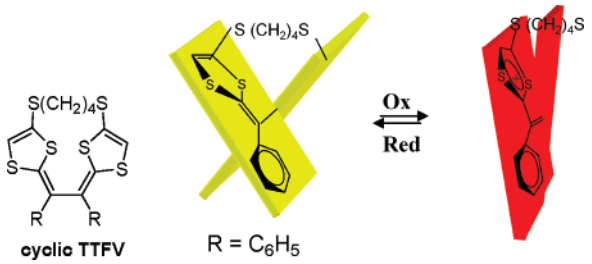

FIGURE 2. Schematic representation of the clip movement observed with some cyclic TTFVs upon oxidation.

the TTFV core (Figure 1).[4] These large and fast reversible structural changes associated with the electron transfer at easily attainable oxidation potentials can be compared to stretch movement.[5]

According to the molecular structure of the TTFVs, a second type of movement can be triggered by electron transfer. Indeed, the presence of a short bisthioalkyl link between the two dithiole rings such as in cyclic TTFVs prevents any stretch motion, and upon oxidation, the two dithiolium rings become closer and a clip movement occurs (Figure 2).[6] It is worth noting that with a longer bisthioalkyl link (e.g., $(CH_2)_{12}$), the motion is similar to that observed in the noncyclic derivative.

Interestingly, the presence of the bisthioalkyl link modifies marginally the donor ability of these molecules compared to the noncyclic one but has an influence on the oxidation processes. For instance, when R = *p*-$MeOC_6H_4$, two close, reversible, monoelectronic transfers occur for **1** and **2c** (A = $(CH_2)_{12}$) while for **2a**,**b** (A = $(CH_2)_3$, $(CH_2)_4$) a bielectronic transfer leads directly to the dication species.[6] The different exchange processes are tightly bound to the different types of molecular movement, so if an external element impedes or delays the stretch motion, the information should be translated by the electrochemical process. In this connection, the introduction of a crown ether moiety attached to each mobile part of the redox-active framework instead of the bisthioalkyl link should not modify the redox answer of the molecule, provided no cation is present. Indeed, crown ethers are well-known as efficient ligands toward various cations depending on the size of the cavity and therefore as the basis for host−guest chemistry.[7−8] To test our hypothesis, we investigated the synthesis of a series of crown ether vinylogous TTFs where a poly(oxyethyl) ligand of variable length is linked via the two phenyl groups to the central conjugation of these cyclic vinylogous TTFs **3**. First, electrochemical and spectroelectrochemical investigations were performed to analyze the influence of the crown ether ligand length on the nature of the molecular movements induced by electron transfer. Molecular geometry optimizations were realized to rationalize the observed experiments. Preliminary experiments on the ligating ability of these crown ether vinylogous TTFs **3** are also reported. Even if the ligating part of the molecule is far from the redox-active center, complexation alters the structural changes and therefore the redox properties.

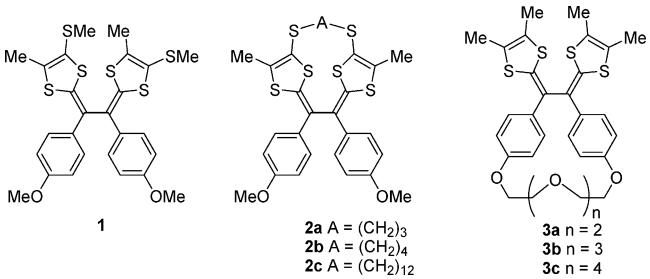

Results and Discussion

The main approach to the synthesis of substituted vinylogous TTFs consists first of the preparation of the 1,4-dithiafulvene derivative and then the formation of the vinylogous TTF core by oxidative coupling of two dithiafulvenyl moieties.[9−10] The

(4) (a) Lorcy, D.; Le Maguerès, P.; Rimbaud, C.; Ouahab, L.; Delhaes, P.; Carlier, R.; Tallec, A.; Robert, A. *Synth. Met.* **1997**, *86*, 1831. (b) Rimbaud, C.; Le Maguerès, P.; Ouahab, L.; Lorcy, D.; Robert, A. *Acta Crystallogr.* **1998**, *C54*, 679. (c) Yamashita, Y.; Tomura, M.; Tanaka, S. Imaeda, K. *Synth. Met.* **1999**, *102*, 1730. (d) Yamashita, Y.; Tomura, M.; Imaeda, K. *Tetrahedron Lett.* **2001**, *42*, 4191. (e) Yamashita, Y.; Tomura, M. *J. Solid State Chem.* **2002**, *168*, 427.

(5) Bellec, N.; Boubekeur, K.; Carlier, R.; Hapiot, P.; Lorcy, D.; Tallec, A. *J. Phys. Chem. A* **2000**, *104*, 9750.

(6) Guerro, M.; Carlier, R. Boubekeur, K.; Lorcy, D.; Hapiot, P. *J. Am. Chem. Soc.* **2003**, *125*, 3159.

(7) (a) Pedersen, C. J. *J. Am. Chem. Soc.* **1967**, *89*, 7017. (b) Gokel, G. W.; Leevy, W. M.; Weber, M. E. *Chem. Rev.* **2004**, *104*, 2723.

(8) Cram, D. J.; Cram, J. M. In *Container molecules and their guests*; Stoddart, J. F., Ed.; RSC, University of Birmingham: Birmingham, U.K., 1994.

(9) (a) Kirmse, W.; Horner, L. *Liebigs Ann. Chem.* **1958**, *614*, 4. (b) Mayer, K.; Kröber, H. *J. Prakt. Chem.* **1974**, *316*, 907. (c) Cava, M. P.; Lakshmikantham, M. V. *J. Heterocycl. Chem.* **1980**, *17*, S39. (d) Schöberl, U.; Salbeck, J.; Daub, J. *Adv. Mater.* **1992**, *4*, 41. (e) Benahmed-Gasmi, A.; Frère, P.; Roncali, J.; Elandaloussi, E.; Orduna, J.; Garin, J.; Jubault, M.; Gorgues, A. *Tetrahedron Lett.* **1995**, *36*, 2983. (f) Bellec, N.; Lorcy, D.; Robert, A.; Carlier, R.; Tallec, A. *J. Electroanal. Chem.* **1999**, *462*, 137.

(10) (a) Fourmigué, M.; Johannsen, I.; Boubekeur, K.; Nelson C.; Batail, P. *J. Am. Chem. Soc.* **1993**, *115*, 3752. (b) Frère, P.; Benahmed-Gasmi, A. S.; Roncali, J.; Jubault, M.; Gorgues, A. *J. Chim. Phys. Phys.-Chim. Biol.* **1995**, *92*, 863. (c) Gonzalez, S.; Martin, N.; Sanchez, L.; Segura, J. L.; Seoane, C.; Fonseca, I.; Cano, F. H.; Sedo, J.; Vidal-Gancedo, J.; Rovira, C. *J. Org. Chem.* **1999**, *64*, 3498. (d) Roncali, J. *J. Mater. Chem.* **1997**, *7*, 2307. (e) Lorcy, D.; Guerin, D.; Boubekeur, K.; Carlier, R.; Hascoat, P.; Tallec, A.; Robert, A. *J. Chem. Soc., Perkin Trans. 1* **2000**, 2719. (f) Hascoat, P.; Lorcy, D.; Robert, A.; Carlier, R.; Tallec, A.; Boubekeur, K.; Batail, P. *J. Org. Chem.* **1997**, *62*, 6086.

SCHEME 1

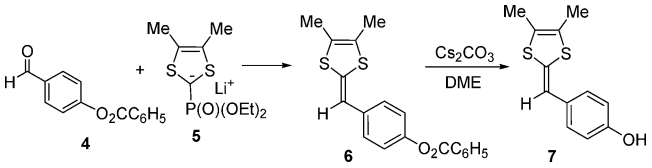

SCHEME 2

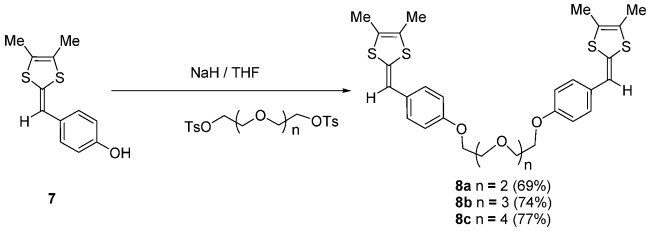

SCHEME 3

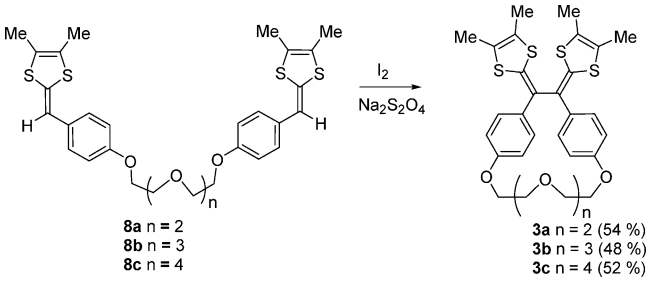

bisdithiafulvenyl derivatives were synthesized according to the chemical pathway described in Scheme 1. Our key material is the dithiafulvene **7** substituted with a *p*-phenol group which is smoothly prepared, starting from *p*-hydroxybenzaldehyde. First, we protected the phenol group with a benzoate moiety to prepare the aldehyde **4**,[11] and the reaction of **4** with the 4,5-dimethyl-1,3-dithiolylphosphonate anion **5**, generated from the 4,5-dimethyl-1,3-dithiolylphosphonate in the presence of BuLi, afforded dithiafulvene **6** in 65% yield. Treatment of **6** with cesium carbonate in refluxing dimethoxyethane (DME)[12] induces the deprotection of the phenol group and the formation of dithiafulvene **7** in excellent yield (90%).

Bis(*p*-toluenesulfonates) of polyethylene glycol with a chain of various lengths, tri-, tetra-, and pentaethylene glycol, were used in the following step. The dithiafulvenylphenol **7** was first treated with sodium hydride in dry THF, and 1/2 equiv of the polyethylene glycol bis(p-toluenesulfonates) was added in dilute conditions (Scheme 2). The corresponding bisdithiafulvenes **8a**−**c** were isolated in good yields after column chromatography.

All the dithiafulvenes **8a**−**c** have been analyzed by cyclic voltammetry in dichloromethane, and their oxidation potentials are listed in Table 1. These derivatives exhibit on the first anodic scan an irreversible oxidation wave, and upon successive scans a reversible system appears at a lower potential than the first oxidation peak. This is classical behavior for dithiafulvenes as, upon oxidation, the radical cation which forms dimerizes to a protonated species, leading, after deprotonation, to the vinylogous TTF.[13] The vinylogous TTFs formed in the medium exhibit

TABLE 1. Redox Potentials of Bisdithiafulvenes 8a−c and TTFV 3a−c[a]

	E_{pa} (V), CH_2Cl_2		E_1, E_2 (V), CH_2Cl_2	E (V), CH_3CN
8a	0.46	**3a**	0.33	0.28
8b	0.47	**3b**	0.31	0.30
8c	0.49	**3c**	0.19, 0.34	0.25

[a] E in volts vs SCE, n-Bu_4NPF_6, Pt, 0.1 M, scanning rate 0.1 V/s.

a reversible oxidation system at a less positive potential than the starting dithiafulvenes. The electrochemical behavior is quite similar for both the monodithiafulvenes **6** and **7** and the bisdithiafulvenes **8a**−**c**. It can be noticed that the E_{pa} values of bisdithiafulvenes **8a**−**c** are not influenced by the chain length and are close to that observed for the dithiafulvene **7** (E_{pa} = 0.46 V vs SCE), while for **6** (E_{pa} = 0.65 V vs SCE) the E_{pa} value is positively shifted due to the presence of the electron-withdrawing effect of the substituent $C_6H_5CO_2$. These electrochemical investigations carried out on the bisdithiafulvenes **8a**−**c** show that upon oxidation two dithiafulvene cores couple into a redox-active vinylogous TTF. However, since electrodeposition occurs at the electrode, forming an insoluble film,[14] we could not perform electrochemical synthesis of the vinylogous TTF, as realized previously for other TTFV derivatives.

To avoid the electrodeposition, we favor the chemical coupling instead of the electrochemical one for the preparation of the vinylogous TTFs **3a**−**c** (Scheme 3). The bisdithiafulvenes **8a**−**c** were oxidized in the presence of iodine, and the solution was then treated with a large excess of $Na_2S_2O_4$.[3g,15] The vinylogous TTFs **3a**−**c** resulting from the intramolecular coupling are isolated as viscous oils. The redox behavior of these derivatives has been analyzed by cyclic voltammetry in acetonitrile and dichloromethane, and their redox potentials are collected in Table 1.

In acetonitrile, it can be noticed that they all present only one reversible bielectronic oxidation wave and that the size of the poly(oxyethyl) chain does not influence significantly the electron-donating properties of the TTFVs **3a**−**c**. Interestingly, in dichloromethane the redox behavior depends on the size of the poly(oxyethyl) chain. For the shorter chains, such as those in **3a** and **3b**, one reversible oxidation wave was observed, while for **3c** two close reversible monoelectronic processes were observed.

This behavior can be compared to what was observed on cyclic vinylogous TTFs **2**, where the two dithiole rings are linked through the outer sulfur atoms with an alkyl chain of various lengths (A = $(CH_2)_3$, $(CH_2)_4$, $(CH_2)_{12}$). All these derivatives exhibited only one reversible bielectronic oxidation wave in acetonitrile, while in dichloromethane the signature of the electroactive species was dependent on the size of the alkyl chain. For the shorter bridging chains (A = $(CH_2)_3$ or $(CH_2)_4$) only one reversible wave was observed; thus, in this case the neutral TTFVs **2a**,**b** are directly oxidized to their dicationic form. Contrariwise, when the bisthioalkyl chain was longer (A = $(CH_2)_{12}$), the redox behavior of **2c** was found to be similar to that of the noncyclic vinylogous TTF **1**, which is two close monoelectronic waves.[3b] The poly(oxyethyl) chain in **3** and the

(11) (a) Staedler, P. A. *Helv. Chim. Acta.* **1978**, *61*, 1675−1680. (b) Greene, T. W.; Wuts, P. G. W. *Protective groups in organic synthesis*, 3rd ed.; Wiley: New York, 1999; see also references cited therein.

(12) Zaugg, H. E. *J. Org. Chem.* **1976**, *41*, 3419.

(13) Hapiot, P.; Lorcy, D.; Tallec, A.; Carlier, R.; Robert, A. *J. Phys. Chem.* **1996**, *100*, 14823.

(14) Massue, J.; Ghilane, J.; Bellec, N.; Lorcy, D.; Hapiot, P. *Electrochem. Commun.* **2007**, *9*, 677.

(15) (a) Müller, H.; Salhi, F.; Divisia-Blohorn, B. *Tetrahedron Lett.* **1997**, *38*, 3215. (b) Lorcy, D.; Rault-Berthelot, J.; Poriel, C. *Electrochem. Commun.* **2000**, *2/6*, 382.

TABLE 2. λ_{max} (nm) Associated with the Different Species Produced upon Oxidation

TTFV	neutral	radical cation	dication
1	335	597, 700	585
3b	344		380
3c	340	585, 704	450

p-MeO substituents in **1** and **2** induce close electronic effects on the aromatic ring, and therefore, the different redox behavior observed here is unambiguously attributable to steric hindrance induced by the size of the poly(oxyethyl) links and can be correlated to molecular movements of opposite nature associated with the electron transfer. Indeed, for the cyclic vinylogous TTFs **2** with short bisthioalkyl links, a fast molecular clip was activated upon electron transfer, while for the longest chain or the noncyclic vinylogous TTF **1**, a stretch movement was induced upon oxidation.[6] Therefore, the redox behavior of the cyclic TTFVs **3a**−**c** appears to be similarly dependent on the size of the bridging poly(oxyethyl) chain. If this link is long enough (**3c**), it will allow a stretch movement upon electron transfer, while if it is shorter, a clip movement occurs (**3a**,**b**).

To confirm the influence of the poly(oxyethyl) chain on the molecular movements, we performed spectroelectrochemical experiments on **3b** and **3c**, where the species produced during exhaustive oxidation are followed by spectral changes and compared with noncyclic TTFV **1**. The absorption values of the neutral, radical cation, and dication species are summarized in Table 2. All the neutral species exhibit similar UV−vis spectra with a $\lambda_{max} \approx 340$ nm, indicating that, with or without the bridging chain, the vinylogous TTF skeletons present the same conformations with no significant influence of the bridge. Actually, the X-ray molecular structure of **1** was previously reported showing nonplanar geometry; thus, a similar spatial arrangement of the electroactive core in **3** can be envisaged.[3b] Analyses of the UV−vis spectra upon oxidation show two different cases (Figure 3). On one hand, with the longest bridging chain such as with **3c** the formation of the radical cation (large peak around 585 nm and absorbance in the 704 nm range) was initially visible before the formation of the dication (only one peak around 450 nm). On the other hand, for **3b** the dication is produced directly with a broad absorption band at $\lambda_{max} \approx$ 380 nm, evidencing a completely different dicationic backbone for the vinylogous TTF core. The spectroelectrochemical experiments confirm that the nature of the molecular movement, and therefore the redox behavior, is influenced by the size of the bridge and that only the poly(oxyethyl) chain in **3c** is long enough to enable a stretch movement as observed in the nonrestrained molecule **1** or **2c** (A = $(CH_2)_{12}$).

By contrast with the noncyclic analogue **1**, the signature of the dicationic species is observed at different wavelengths (450 nm for **3c** and 585 nm for **1**). As already mentioned above, the dicationic species of TTFV $\mathbf{1}^{2+}$ has been characterized by X-ray diffraction analysis and the vinylogous TTF skeleton was proved to be planar. Therefore, the hypsochromic shift of λ_{max} observed for the absorption band of the dicationic species $\mathbf{3c}^{2+}$ might indicate a slightly distorted dicationic conformation.

To get additional information on the neutral and the dicationic states of the TTFVs **3a**−**c**, we used molecular modeling calculations to determine their geometries. As previously reported for cyclic and noncyclic TTFVs, when the X-ray structure is obtained, molecular modeling based on DFT (density functional theory) gives good agreement between the X-ray data and calculated conformations for cyclic and noncyclic TTFVs. Therefore, calculations could provide useful information on the molecular geometries of **3a**−**c** since we did not obtain crystals of these derivatives. As can be seen in Figure 4, the chain link does not considerably affect the geometry of the molecules at the neutral state. However, when the TTFVs **3a**−**c** are viewed along the central C−C axis (Figure 4, bottom), the molecular geometry seems slightly more constrained with the shortest link, TTFV **3a**. The acute dihedral angle based on this central C−C bond for the two dithiole rings in **3a**, **3b**, and **3c** increases with the length of the crown ether chain and amounts to 61.0°, 66.7°, and 68.1°, respectively. The comparison of these angle values to that observed in the neutral structure of **1**, which amounts to 74(1)°, evidences the strain release from **3a** to **3b**, while the further addition of one oxyethyl spacer in **3c** moderately influences the value of this angle.

As far as the dicationic forms are concerned, two isomers were obtained depending on the length of the poly(oxyethyl) chain. For $\mathbf{3a}^{2+}$ and $\mathbf{3b}^{2+}$ the calculations evidence the *Z* isomer on the central C═C double bond with the two dithiolium rings on the same side resulting from a clip movement, whereas for $\mathbf{3c}^{2+}$, the *E* isomer is obtained with the two dithiolium rings on each side of the central double bond resulting from a stretch movement. The evolution of the acute dihedral angles based

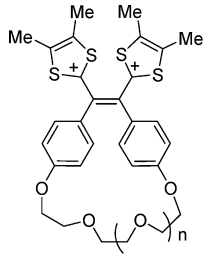

Z for 3a 3b

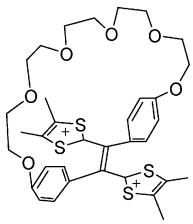

E for 3c

on this central C═C bond for the two dithiole rings in $\mathbf{3a}^{2+}$ and $\mathbf{3b}^{2+}$ amounts to 46.9° and 51.1°, respectively, evidencing a decrease of the value of this angle in the dicationic species compared to those observed in the neutral species. In **3c**, the poly(oxyethyl) chain is long enough to allow an opening out of the molecule evidenced by the fact that $\mathbf{3c}^{2+}$ exhibits an acute dihedral angle of 154.8° (Figure 5C). Moreover, compared to the 180° expected for a planar geometry of the TTFV core and observed in $\mathbf{1}^{2+}$,[4b] the slightly folded structure obtained for $\mathbf{3c}^{2+}$ is in agreement with the hypsochromic shift of λ_{max} noticed during the spectroelectrochemical experiments above.

All these experiments, electrochemical and spectroelectrochemical, and calculations support the fact that the presence of at least a hexakis(oxyethyl) chain connecting the two aromatic rings on the *para* position of the TTFV is necessary to allow a stretch movement upon oxidation in the case of **3**.

Poly(oxyethyl) chains are well-known for complexing a large variety of cations depending on the sizes of the cation and the poly(oxyethyl) chain.[16] Several redox-active moieties such as ferrocene[17] or tetrathiafulvalene[18] have been functionalized with

(16) Boulas, P. L.; Gomes-Kaifer, M.; Echegoyen, L. *Angew. Chem., Int. Ed.* **1998**, *37*, 216.

(17) (a) Beer, P. D.; Gale, P. A.; Zheng, Cheng G. *Coord. Chem. Rev.* **1999**, *185*−*186*, 3. (b) Miyaji, H.; Collinson, R. S.; Prokes, I. *Chem. Commun.* **2003**, *1*, 64. (c) Oton, F. O.; Tarraga, A.; Velasco, D. M.; Molina, P. *Dalton Trans.* **2005**, *7*, 1159.

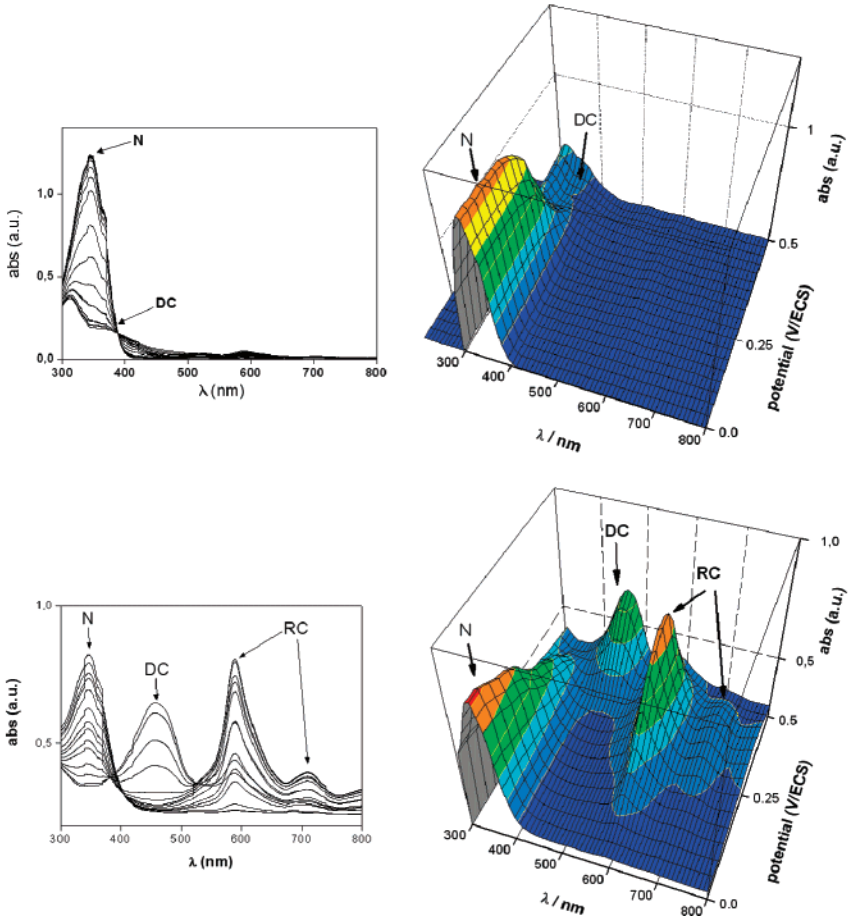

FIGURE 3. UV−vis spectroelectrochemistry of **3b** (5×10^{-4} M) (top) and **3c** (5×10^{-4} M) (bottom) in CH_2Cl_2 (0.2 M Bu_4NPF_6). Oxidation on a platinum grid (N = neutral, RC = radical cation, DC = dication).

either crown ether or acyclic receptors to make receptors capable of electrochemically monitoring the complexation of the cations. In the case of TTF-derived receptors, the recognition, monitored by cyclic voltammetry, usually results in a positive shift of the first redox potential due to the binding of the positively charged ion in close vicinity of the TTF core. However, as soon as the ether ligand is not directly linked to the donor core, via for instance a phenyl ring, only a very weak positive shift ($\Delta E <$ 10 mV) of the first oxidation process associated with the complexation can be detected by cyclic voltammetry, due to a lack of communication between the receptor and the electroactive unit.[19] Basically, a similar situation can be envisioned with TTFV **3**, where the poly(oxyethyl) chain could also behave as a ligand toward guest cations, but the fact that the binding site is located far away from the redox-active core should render the electrostatic repulsion usually observed in simple TTF receptors negligible.

Complexation studies have been performed on TTFVs **3a**−**c** using cyclic voltammetry by adding aliquots of test guest cations solubilized in CH_3CN. Several cations have been tested such as Li^+, Na^+, K^+, Cd^{2+}, Pb^{2+}, and Ba^{2+}. If the studies are performed in acetonitrile, no significant modification of the voltammograms of **3a**−**c** is observed, regardless of the tested cations. Similarly, using a dichloromethane solution of **3a**,**b**, no modifications of the cyclic voltammograms are observed. Actually, only the cyclic voltammograms of the TTFV **3c** exhibit some modifications in the presence of Pb^{2+} (Figure 6A). As shown above, in the absence of cation, TTFV **3c** exhibits the classical two-reversible-wave behavior. After progressive aliquot addition of Pb^{2+}, the first oxidation wave becomes broader and the anodic peak potential E_{pa} is shifted to more positive values whereas the corresponding cathodic peak potential E_{pc} is negatively shifted. In fact, the modification mainly affects the peak to peak separation ($\Delta E_p = E_{pa} - E_{pc}$) which passes from 65 to 185 mV between curves a and d and not the midpoint value that is characteristic of the redox potential of the couple ($E° = (E_{pa} + E_{pc})/2$), which changes by around 10 mV. It is noticeable that these modifications are observed for a low ratio of Pb^{2+} to **3c**. When the Pb^{2+} ratio is higher than 0.2 equiv, the complex formed in situ becomes insoluble in dichloromethane and a precipitate in the medium is observed. This suggests that one Pb^{2+} is presumably ligated to more than one redox-active TTFV, inducing the precipitation of the aggregate.[19] This unexpected feature unfortunately impedes the in-depth investigations of the process through either electrochemical or solution ^1H NMR studies.[20]

In other words, the effect of the addition is consistent with a decrease of the electron-transfer rate constant k_s, which varies

(18) (a) Le Derf, F.; Mazari, M.; Mercier, N.; Levillain, E.; Trippé, G.; Riou, A.; Richomme, P.; Becher, J.; Garin, J.; Orduna, J.; Gallego-Planas, N.; Gorgues, A.; Salle, M. *Chem.—Eur. J.* **2001**, *7*, 447. (b) Lyskawa, J.; Le Derf, F.; Levillain, E.; Mazari, M.; Salle, M.; Dubois, L.; Viel, P.; Bureau, C.; Palacin, S. *J. Am. Chem. Soc.* **2004**, *126*, 12194. (c) Lyskawa, J.; LeDerf, F.; Levillain, E.; Mazari, M.; Salle, M. *Eur. J. Org. Chem* **2006**, *10*, 2322. (d) Delogu, G.; Fabbri, D.; Dettori, M. A.; Salle, M.; LeDerf, F.; Blesa, M. J.; Allain, M. *J. Org. Chem.* **2006**, *71*, 9096.

(19) Beer, P. D.; Danks, J. F.; Hesek, D. *Polyhedron* **1995**, *14*, 1327.

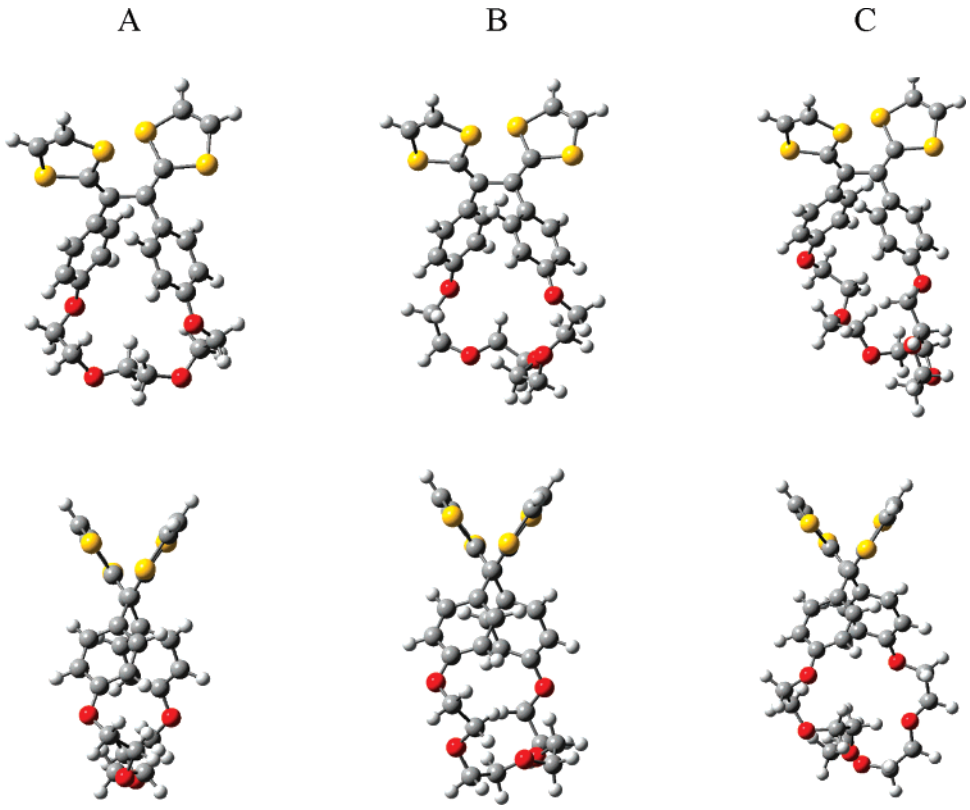

FIGURE 4. Optimized geometries calculated at the B3LYP/6-31G* level of the neutral cyclic TTFV derivatives **3a** (A), **3b** (B), and **3c** (C).

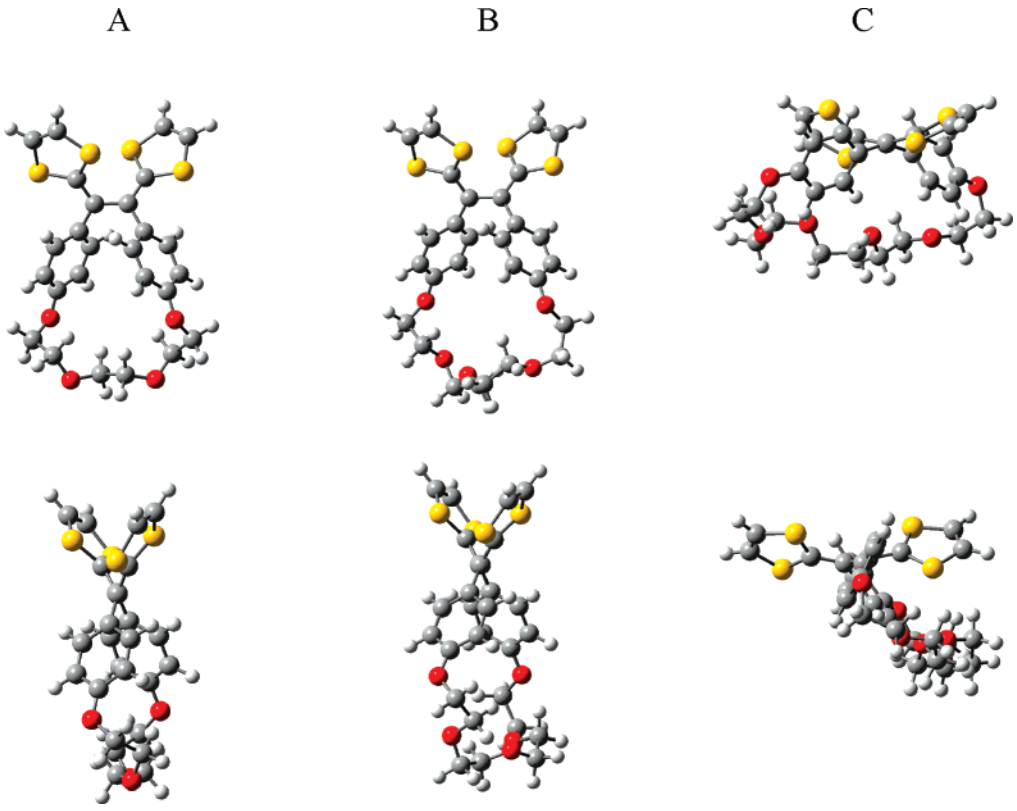

FIGURE 5. Optimized geometries calculated at the B3LYP/6-31G* level of the dicationic cyclic TTFV derivatives $\mathbf{3a}^{2+}$ (A), $\mathbf{3b}^{2+}$ (B), and $\mathbf{3c}^{2+}$ (C).

by at least 1.5 orders of magnitude and has very little effect on the thermodynamics (variation of $E°$). It is also noticeable that the second wave remains almost unmodified, which indicates that a possible passivation of the electrode surface is likely not responsible for the kinetics decrease. Also directed to this end, the peak to peak separation of the first transfer increases with

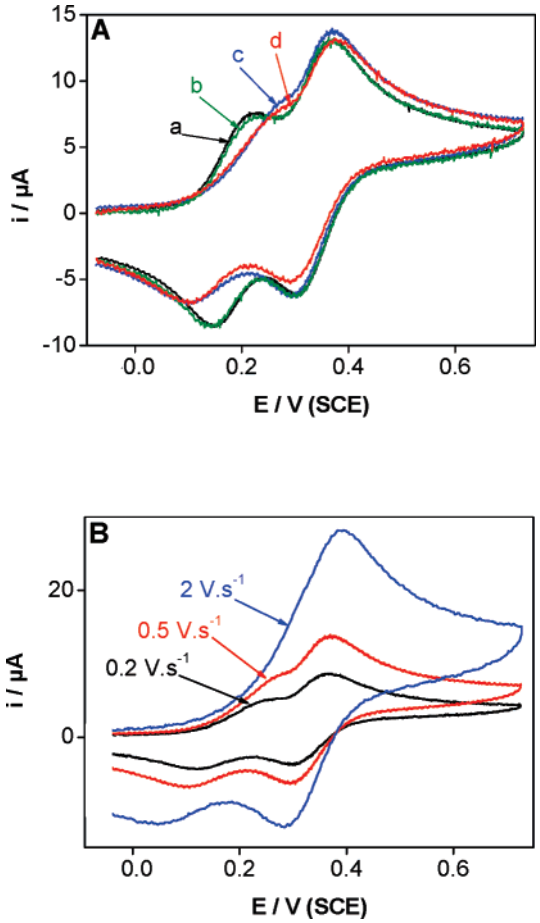

FIGURE 6. Voltammograms of TTFV **3c** (1.4×10^{-3} M) in CH_2Cl_2 with 0.1 M *n*-Bu_4NPF_6 (A) at a 0.5 V/s scan rate in the presence of increasing amounts of Pb^{2+}($Pb(ClO_4)_2$) [(a) without $Pb(ClO_4)_2$, (b) 0.05 equiv of $Pb(ClO_4)_2$, (c) 0.1 equiv of $Pb(ClO_4)_2$, (d) 0.15 equiv of $Pb(ClO_4)_2$] and (B) with 0.15 equiv of $Pb(ClO_4)_2$ at different scan rates.

the scan rate from 0.2 to 2 V/s in the presence of 0.15 equiv of $Pb(ClO_4)_2$ (Figure 6B). This behavior is clearly different from those previously reported when complexation occurs. Generally, the addition of a cation in a solution containing the electroactive molecules bearing a crown ether moiety results in a modification of the apparent oxidation potential, i.e., of the electron-transfer thermodynamics due to the existence of fast equilibrium. To explain our observations, we should recall some previous results concerning the factors controlling the activation energy of the electron transfer. For similarly hindered TTFVs, we found that the molecular movement is concerted with the electron transfer, which implies that the "extra" reorganization energy due to the conformational changes is part of the total activation energy of the electron transfer, and we have shown that most of the molecular movement occurs during the first electron transfer.[5] Experimentally, for **3c** the presence of the molecular modification is visible from the lower rate constant measured for the first electron transfer than the value for the second one; k_s = 0.035 cm·s^{-1} and k_s = 0.12 cm·s^{-1}, respectively, for the first and the second electron-transfer processes.[21] Indeed, in the framework of the Marcus−Hush model,[22,23] the reorganization free energy of the electron transfer λ_{elec} is composed of a solvent reorganization term, $\lambda_{0,elec}$, and an intramolecular reorganization term, $\lambda_{i,elec}$, $\lambda_{elec} = \lambda_{0,elec} + \lambda_{i,elec}$. The electrochemical standard rate constant k_s, which characterizes the electron-transfer kinetics, is then derived from the reorganization terms:

$$k_s = Z^{el} \exp\left[-\frac{F(\lambda_{0,elec} + \lambda_{i,elec})}{4RT}\right]$$

with $Z^{el} = (RT/2\pi M)^{1/2}$ (M = molar mass) and $\lambda_{0,elec} = 3/a$ (a = radius of the equivalent sphere, Å). $\lambda_{0,elec}$ characterizes the solvent reorganization and should not be considerably modified by the complexation. On the contrary, we can postulate that when the lead cation is complexed by the crown ether ring in the neutral TTFV **3c**, this complexation brings some more rigidity to the molecule that will mainly affect the molecular movement and thus $\lambda_{i,elec}$. The origin of the effects is thus different from that of the "classical cases reported in the litterature". Here the complexation is not visible because of some electrostatic interactions between the TTFV and the cation which affect the stability of the reduced and oxidized species and thus the apparent $E°$, but we can propose that complexation induces an increase of the rigidity and thus a higher activation energy of the concerted electron transfer with the conformational changes. Considering the estimation of the k_s variation, the change of the activation energy, due to the higher rigidity of the molecular framework, can be estimated to be on the order of 0.3 eV.

Conclusion

A series of vinylogous TTFs bearing a crown ether binding site of variable length have been synthesized. Both spectroelectrochemistry and molecular modeling based on DFT support the fact that a crown ether chain comprised of six oxygens is necessary to obtain a stretch movement of the TTFV core upon oxidation. Complexation studies have been undertaken on these derivatives, and preliminary results suggest that the recognition process involves both selectivity and sensitivity. Indeed, the TTFV bearing the longest crown ether chain (composed of six oxygens) is the only one in the series synthesized to provide an optimal coordination environment for Pb^{2+} cations. Besides, the low concentrations of Pb^{2+} involved in the complexation process suggest a high sensitivity of these receptors for cations, which might be due to the rigidification of the crown ether ring after complexation. This rigidification appears as a decrease of the apparent electron-transfer kinetics and has little effect on the thermodynamics as the crown ether is far from the redox center. Unfortunately, the lack of solubility of the metallic salts in dichloromethane limits deeper investigations, as the complex formed in situ precipitates out in the medium after addition of 0.2 equiv of Pb^{2+}. Current investigations are in progress to synthesize new crown ether based receptors which would exhibit

(20) At this lead concentration, a voltammogram with two distinct waves similar to the first voltammogram obtained without lead but with this time a lower current is observed. As the complex formed between TTFV **3c** and Pb^{2+} precipitates in the medium, the only electroactive species in solution is some uncomplexed TTFV **3c**.

(21) (a) Assuming the Buttler−Volmer law, a transfer coefficient of α = 0.5, and a value for the diffusion coefficient $D = 10^{-5}$ cm·s^{-1}. (b) Savéant, J.-M. *Elements of molecular and biomolecular electrochemistry: an electrochemical approach to electron transfer chemistry*; Wiley-Interscience: Hoboken, NJ, 2006.

(22) (a) Marcus, R. A. J. *Chem. Phys.* **1956**, *24*, 966. (b) Marcus, R. A. *J. Chem. Phys*. **1956**, *24*, 979. (c) Hush, N. S. *J. Chem. Phys*. **1958**, *28*, 962. (d) Hush, N. S. *Trans. Faraday Soc*. **1961**, *57*, 557. (e) Marcus, R. A. J. *Chem. Phys*. **1965**, *43*, 679.

(23) Kojima, H.; Bard, A. J. *J. Am. Chem. Soc*. **1975**, *97*, 6317.

a better solubility in dichloromethane, especially when a cation is inserted inside the complexing cavity, and would allow the in-depth investigation of the process.

Experimental Section

Dithiafulvene 6. To a solution of dithiole phosphonate **5** (1 g, 3.73 mmol) in 80 mL of freshly distilled anhydrous THF was added dropwise *n*-BuLi (2.57 mL, 4.1 mmol, of a 1.6 M solution in hexane) at −78 °C under an inert atmosphere. After the resulting solution was stirred for 20 min at −78 °C, a solution of 4-formylphenyl benzoate (**4**; 928 mg, 4.1 mmol) in 5 mL of THF was added. The reaction mixture was then allowed to reach room temperature and stirred for an additional 12 h. The solvent was then removed under vacuo, and 60 mL of CH_2Cl_2 was added to the residue. The organic phase was washed with water and dried over $MgSO_4$, and the solvent was evaporated. After chromatography on silica gel using dichloromethane/*n*-pentane (1:1) as eluent, the dithiafulvene **6** was obtained as a yellow powder (824 mg, 65%): mp 164 °C; ^{1}H NMR ($CDCl_3$, 300 MHz) δ 2.01 (s, 6H, CH_3), 6.48 (s, 1H, CH), 7.21−7.26 (m, 4H, CHAr), 7.51−7.68 (m, 3H, CHAr), 8.23−8.27 (m, 2H, CH Ar); ^{13}C NMR ($CDCl_3$, 75 MHz) δ11.8, 12.6 109.5, 119.9, 120.0, 120.6, 126.3, 127.4, 128.5, 129.1, 132.5, 133.4, 133.9, 146.9, 164.1 IR (KBr; ν, cm^{-1}) 1732 (C═O); HRMS (EI, *m/z*) calcd for $C_{19}H_{16}O_2S_2$ 340.0591, found 340.0581. Anal. Calcd for $C_{19}H_{16}O_2S_2$: C, 67.03; H, 4.74; S, 18.84. Found: C, 67.11; H, 4.74; S, 18.08.

Dithiafulvene 7. Cs_2CO_3 (1.24 g, 3,82 mmol) was added to a stirred solution of dithiafulvene **6** (1 g, 2.94 mmol) in 40 mL of dimethoxyethane. The reaction mixture was refluxed for 24 h, and the solvent was removed under vacuum. The residue was dissolved in 60 mL of CH_2Cl_2, washed with water (3 × 50 mL), and dried over $MgSO_4$. After removal of the solvents, column chromatography of the crude product on silica gel with dichloromethane/*n*-pentane (1:1) as the eluent afforded **7** as a beige powder (694 mg, 90%): mp 139 °C; ^{1}H NMR ($CDCl_3$, 200 MHz) δ 1.98 (s, 6H, CH_3), 5.24 (s, 1H, OH), 6.40 (s, 1H, CH) 6.86 (d, 2H, CHAr) 7.18 (d, 2H, CH Ar); ^{13}C NMR ($CDCl_3$, 50 MHz) δ 14.08, 13.4, 111.8, 115.8, 128.4, 121.1, 130.0, 130.7, 131.6, 153.4; HRMS (EI, *m/z*) calcd for $C_{12}H_{12}OS_2$ 236.0329, found 236.0321. Anal. Calcd for $C_{12}H_{12}OS_2$: C, 61.02; H, 5.08; S, 27.12. Found: C, 60.93; H, 5.17; S, 26.78.

General Procedure for the Synthesis of Bisdithiafulvenes 8a−c. NaH (186 mg, 4.66 mmol) was added to a solution of dithiafulvene **7** (1 g, 4.23 mmol) in 40 mL of distilled THF. The reaction mixture was refluxed for 1 h, and the appropriate tosylate was then added (1.9 mmol, 870 mg for **8a**, 955 mg for **8b**, and 1.04 g for **8c**) in 5 mL of THF. The solution was refluxed for an additional 24 h. After removal of the solvent, 60 mL of dichloromethane was added. The organic phase was washed with water (3 × 50 mL) and dried over $MgSO_4$. After column chromatography on silica gel using dichloromethane/*n*-pentane (1:1) as the eluent, the bisdithiafulvenes were obtained as a viscous oil.

Data for compound 8a: yield 69%; R_f = 0.42; ^{1}H NMR ($CDCl_3$, 300 MHz) δ 1.84 (s, 12H, CH_3), 3.65 (s, 4H, CH_2), 3.74−3.77 (m, 4H, CH_2), 4.00−4.03(m, 4H, CH_2), 6.26 (s, 2H, CH), 6.79 (d, 4H, CH Ar), 7.07 (d, 4H, CH Ar); ^{13}C NMR ($CDCl_3$, 75 MHz) δ 11.9, 12.6, 66.4, 68.8, 69.8, 110.5, 113.6, 119.5, 119.7, 126.7, 129.6, 130.1, 155.3; HRMS (ESI, *m/z*) calcd for $C_{30}H_{34}O_4S_4$ [M + H] 587.1418, found [M + H]$^{\bullet+}$ 587.1387. Anal. Calcd for $C_{30}H_{34}O_4S_4$: C, 61.40; H, 5.84. Found: C, 61.33; H, 6.08.

Data for compound 8b: yield 74%; R_f = 0.38; ^{1}H NMR ($CDCl_3$, 300 MHz) δ 1.94 (s, 6H, CH_3), 1.95 (s, 6H, CH_3), 3.72 (m, 8H, CH_2), 3.85 (m, 4H, CH_2), 4.13 (m, 4H, CH_2), 6.38 (s, 2H, CH), 6.91 (d, 4H, CH Ar) 7.18 (d, 4H, CH Ar); ^{13}C NMR ($CDCl_3$, 75 MHz) δ 13.3, 14.1, 67.9, 70.2, 71.1, 71.2, 121.0, 121.1, 111.8, 115.1, 128.1, 130.7, 131.5, 156.8; HRMS (*m/z*) calcd for $C_{32}H_{38}O_5S_4$ [M + Na]$^+$ 653.1500, found 653.1492. Anal. Calcd for $C_{32}H_{38}O_5S_4 \cdot 0.75CH_2Cl_2$: C, 56.64; H, 5.69. Found: C, 56.70; H, 5.77.

Data for compound 8c: yield 77%; R_f = 0.30; ^{1}H NMR ($CDCl_3$, 300 MHz) δ 1.93 (s, 6H, CH_3), 1.94 (s, 6H, CH_3), 3.70 (m, 12H, CH_2), 3.84 (m, 4H, CH_2), 4.12 (m, 4H, CH_2), 6.36 (s, 2H, CH), 6.89 (d, 4H, CH Ar), 7.16 (d, 4H, CH Ar); ^{13}C NMR ($CDCl_3$, 75 MHz) δ 11.9, 12.6, 66.4, 68.7, 69.6, 69.7, 110.3, 113.6, 119.6, 119.7, 126.7, 129.2, 130.1, 155.3; HRMS (*m/z*) calcd for $C_{34}H_{42}O_6S_4$ [M + H] 675.1943, found [M + H]$^{\bullet+}$ 675.1934. Anal. Calcd for $C_{34}H_{42}O_6S_4 \cdot 0.33CH_2Cl_2$: C, 58.84; H, 5.81. Found: C, 58.56; H, 5.68.

General Procedure for the Synthesis of Cyclic Vinylogous TTFs 3a−c. To a solution of the bisdithiafulvene **8** (1 mmol, 586 mg for **8a**, 630 mg for **8b**, and 674 mg for **8c**) in 40 mL of dichloromethane under an inert atmosphere was added I_2 (750 mg, 3 mmol), and the medium was heated to reflux for 8 h. To the solution was added a large excess of $Na_2S_2O_4$ (2 g) to reduce the dicationic TTFV formed in the medium. The reaction mixture was refluxed overnight and allowed to reach room temperature. After filtration of the suspension, the filtrate was washed with water (2 × 50 mL) and dried over $MgSO_4$, and the solvent was removed under vacuum. The TTFVs **3a−c** were purified by column chromatography on silica gel using ethyl acetate as the eluent and obtained as waxy compounds.

Data for compound 3a: yield 54%; ^{1}H NMR ($CDCl_3$, 300 MHz) δ 1.94 (s, 12H, CH_3), 3.60 (s, 4H, CH_2), 3.75−3.79 (m, 4H, CH_2), 4.11−4.19 (m, 4H, CH_2), 6.71 (d, 4H, CH Ar), 7.14 (d, 4H, CH Ar); ^{13}C NMR ($CDCl_3$, 75 MHz) δ 12.9, 13.7, 67.3, 69.8, 70.8, 112.1, 114.5, 115.9, 121.2, 122.0, 127.7, 130.4, 157.3; HRMS (*m/z*) calcd for $C_{30}H_{32}O_4S_4$ 584.1184, found 584.1163.

Data for compound 3b: yield 48%; ^{1}H NMR ($CDCl_3$, 300 MHz) δ 1.86 (s, 12H, CH_3) 3.25−3.42 (m, 4H, CH_2) 3.65−4.05 (m, 8H, CH_2) 4.20−4.22 (m, 4H, CH_2) 6.82 (d, 4H, CH Ar) 7.32 (d, 4H, CH Ar); ^{13}C NMR ($CDCl_3$, 75 MHz) δ 12.3, 13.1, 66.8, 67.7, 68.7, 69.6, 113.5, 114.5, 119.5, 126.9, 128.8, 130.5, 132.8, 155.8; HRMS (ESI, *m/z*) calcd for $C_{32}H_{36}O_5S_4$ 628.1446, found 628.1487, and calcd for $C_{32}H_{36}O_5NaS_4$ 651.1343, found 651.1345.

Data for compound 3c: yield 52%; ^{1}H NMR ($CDCl_3$, 300 MHz) δ 1.97 (s, 12H, CH_3), 3.41 (s, 4H, CH_2), 3.48 (m, 4H, CH_2), 3.61 (m, 4H, CH_2), 3.78 (m, 4H, CH_2), 4.18 (m, 4H, CH_2), 6.85 (d, 4H, CH Ar), 7.40 (d, 4H, CH Ar); ^{13}C NMR ($CDCl_3$, 75 MHz) δ 13.3, 13.8, 67.8, 69.9, 70.4, 70.5, 70.8, 115.1, 120.9, 122.3, 123.2, 127.9, 131.0, 134.2, 156.9; HRMS (ESI, *m/z*) calcd for $C_{34}H_{40}O_6S_4$ 672.1707, found 672.1717.

Supporting Information Available: ^{1}H and ^{13}C NMR spectra of **3a−c** and **8a−c**, HRMS spectrum of **3b**, drawings of the optimized geometries at the B3LYP/6-31G* level, values of the energies in hartrees, and the Cartesian coordinates for the neutrals and dications of the investigated TTFVs **3a−c**. This material is available free of charge via the Internet at http://pubs.acs.org.

JO0701841